

Photo- and Radiation-Chemical Formation and Electrophilic and Electron Transfer Reactivities of Enolether Radical Cations in Aqueous Solution

Klaus Bernhard,^[a] Judith Geimer,^[b] Moises Canle-Lopez,^[c] Johannes Reynisson,^[a] Dieter Beckert,^[b] Rolf Gleiter,^[d] and Steen Steenken*^[a]

Abstract: In aqueous solution, enolether radical cations (EE⁺) were generated by photoionization ($\lambda \leq 222$ nm) or by electron transfer to radiation-chemically produced oxidizing radicals. Like other radical cations, the EE⁺ exhibit electrophilic reactivity with respect to nucleophiles such as water or phosphate as well as electron transfer reactivity, for example, towards one-electron reductants such as phenols, amines, vitamins C and E, and guanine nucleosides. The

reactivity of these electron donors with the radical cation of *cis*-1,2-dimethoxyethene⁺ (DME⁺) can be described by the Marcus equation with the reorganization energy $\lambda =$

16.5 kcal mol⁻¹. By equilibrating DME⁺ with the redox standard 1,2,4-trimethoxybenzene, the reduction potential of DME⁺ is determined to be 1.08 ± 0.02 V/NHE. The oxidizing power of the radical cation of 2,3-dihydrofuran, which can be considered a model for the enolether formed on strand breakage of DNA, is estimated to be in the range 1.27–1.44 V/NHE.

Keywords: density functional calculations • DNA • electron paramagnetic resonance • ionization potential • photoionization • redox potential

Introduction

Enolether radical cations (EE⁺) are of interest because a) they belong to the simplest π -type systems and b) because they are formed in heterolytic β -fragmentation reactions^[1] involving α -alkoxyalkyl radicals, the best-known and most important example being the C4'-radical in DNA, whose heterolysis^[2–4] is shown in Scheme 1, step a.

From the products isolated, it was concluded^[2] that the radical cation reacts as an electrophile (Scheme 1, step b). The other characteristic, “classical” reaction of radical cations, that is, to act as one-electron acceptors (oxidants),^[5] was discovered in the enolether case almost twenty years later

when it was found that this type of reaction occurs intramolecularly in DNA,^[4, 6] whereby the most easily oxidized nucleobase,^[7] guanine, serves as the electron donor as shown in Scheme 2.

Of course, the nucleophilic addition of water (Scheme 1, step b) competes with this electron transfer reaction. Herein, we try to answer the obvious question as to the dependence on the structure obtained on the electrophilic or one-electron-transfer properties of a family of enolether radical cations, produced in aqueous solution by photo- or radiation-chemical techniques.^[8] In two cases, also a third reaction channel of radical cations, deprotonation, was observed to take place.

Results and Discussion

The cyclic and open-chain enolethers (EE) studied are presented in Scheme 3. In aqueous solution, the enolether function has an absorption band at 195–205 nm (see Figure 1 for an example), which has been interpreted^[9] as originating from a $\pi-\pi^*$ transition.

Gas-phase ionization potentials

Gas-phase ionization potentials of EE, as measured by using photoelectron spectroscopy (PES), are collected in Table 1. The data in Table 1 reveal there is a drastic decrease in ionization potential (IP) on going from an alkene to an enolether. The phenyl group on the double bond reduces the

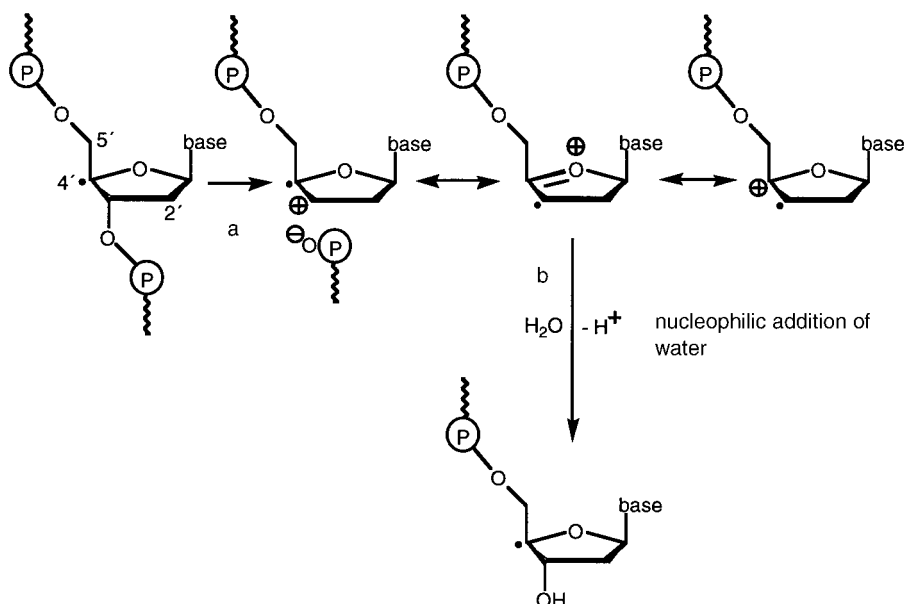
[a] Prof. Dr. S. Steenken, Dipl.-Chem. K. Bernhard, Dr. J. Reynisson
Max-Planck-Institut für Strahlenchemie
45413 Mülheim (Germany)
Fax: (+49)208-306-3951

[b] Dr. J. Geimer, Prof. D. Beckert
Zeitaufgelöste Spektroskopie
Universität Leipzig Permoserstrasse 15
04303 Leipzig (Germany)

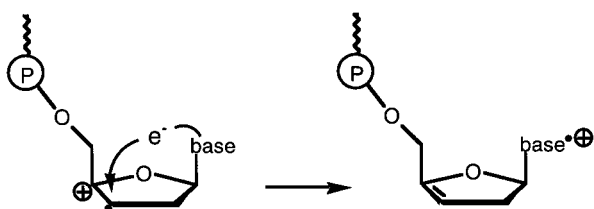
[c] Dr. M. Canle-Lopez
University of La Coruna
15008 A Coruna (Spain)

[d] Prof. Dr. R. Gleiter
Universität Heidelberg
Im Neuenheimer Feld 270
69120 Heidelberg (Germany)

Supporting information for this article is available on the WWW under <http://www.wiley-vch.de/home/chemistry/> or from the author.



Scheme 1. Heterolysis of the C4' radical in DNA. See text for details.



Scheme 2. Reaction of radical cations as one-electron acceptors that occurs intermolecularly in DNA.

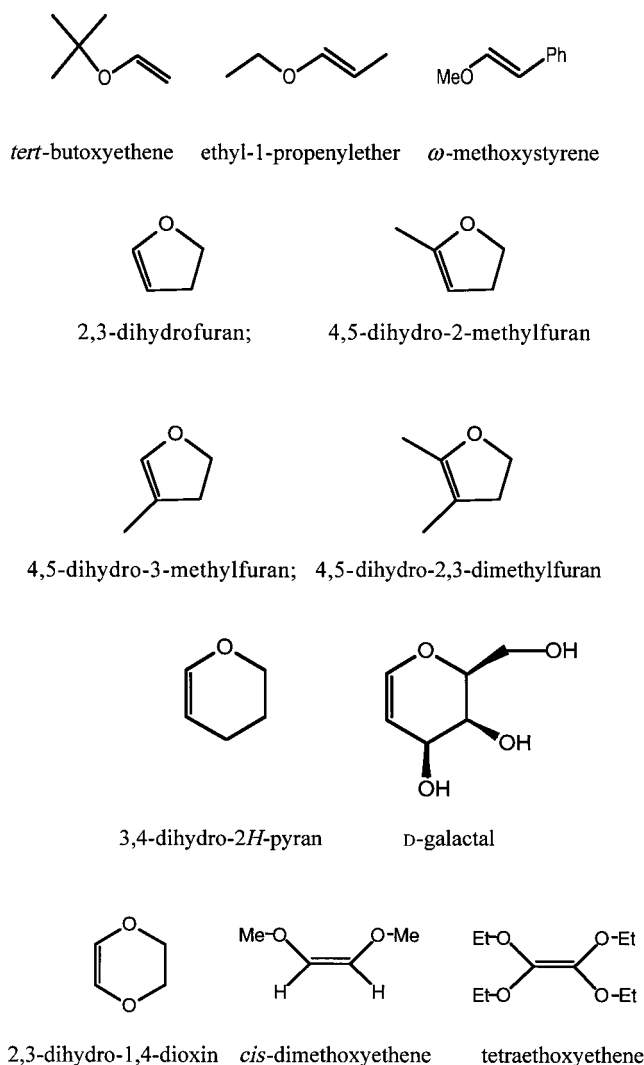
IP considerably. A somewhat weaker but still visible effect is exerted by a second alkoxy group on the double bond, such as in dimethoxyethene or 2,3-dihydro-1,4-dioxin. As expected, the IPs also decrease with methylation at the olefinic bond, as seen from the couple *tert*-butoxyethene/ethyl-1-propenylether and from the dihydrofuran (DHF) family. With the latter, the position of the methyl group on the double bond has no influence on the IP (which is in contrast to the effect on the lifetime of the corresponding radical cation, see column 5 of Table 1). Going from the five-membered ring (furan) to the six-membered pyran ring, the IP decreases, but the effect of the endocyclic methylene group is smaller than that of an exocyclic methyl group (see DHF family). Very strong is the effect of replacing hydrogen atoms by the electron-withdrawing (inductive effect) OH groups (compare dihydropyran/galactal).

Production of radical cations EE^{•+}

Photoionization of enoethers: Photolyzing aqueous solutions of enoethers with the 20 ns pulses from a 193 nm or 222 nm excimer laser generated strong signals from the hydrated electron, e⁻_{aq}. Examples for this are shown in Figure 2 and Figure 3, in which the broad band extending up and above 700 nm is that of e⁻_{aq}, as was confirmed by reaction with typical electron scavengers such as O₂, 2-chloroethanol (see Figure 3), or chloromethane.

In the experiments subsequently described, photolysis with 222 nm light was preferred over that of 193 nm (only) because at 222 nm photoionization can be performed in the presence of e⁻ scavengers such as chloroalkanes which is not possible at 193 nm due to their strong absorption at this wavelength.

At 193 and 222 nm, for all the enoethers the yield of e⁻_{aq} increased linearly with increasing laser power (see inset of Figure 3 for examples); the photoionization process requires just one photon, that is, it is monophotonic. This was the case even for the *least* easily ionized enoether studied, namely *tert*-butoxyethene which has a gas-



Scheme 3. Cyclic and open-chain enoethers discussed in this study.

Table 1. Ionization potentials, photoionization quantum yields $\Phi(e^-)$ of enoethers (EE), and formation (by $\text{Br}_2^{\cdot-}$) and decay rates of EE^+ in water.

EE	IP ^[a] [eV]	$\Phi(e^-)_{222\text{ nm}}$ ^[b]	$k(\text{Br}_2^{\cdot-} + \text{EE})$ [$\text{M}^{-1}\text{s}^{-1}$]	$k(\text{EE}^+ + \text{H}_2\text{O})$ [s^{-1}] at $20 \pm 2^\circ\text{C}$ (from conductance)
ethene ^[c]	10.51 ^[d]			
propene ^[c]	9.73 ^[d]			
methoxyethene	8.93, ^[d] 8.47, ^[e] 8.19 ^[e,f]			
<i>tert</i> -butoxyethene	8.80 ^[e]	0.15	1.3×10^8	$> 5 \times 10^7$
ethyl-1-propenylether	8.53 ^[e]	0.17	4.1×10^8	2.4×10^7
<i>trans</i> - ω -methoxystyrene	8.00 ^[e]	0.12	9.2×10^8	2.8×10^6
<i>cis</i> -dimethoxyethene (DME)	8.27 ^[e]	0.08	1.5×10^9	7.5×10^3 ; 1×10^4 ; ^[h] 6.4×10^3 ^[i]
2,3-dihydro-1,4-dioxin	8.07 ^[d]	0.07	1.5×10^9	1.3×10^4
tetraethoxyethene	7.80 ^[e]	0.11	7.2×10^8	5×10^5
2,3-dihydrofuran (DHF)	8.55, ^[e] 8.5, ^[j] 8.11, ^[e] 7.88 ^[e,f]	0.12	7.7×10^8	1.2×10^7
4,5-dihydro-2-methylfuran (2-MeDHF)	8.19, ^[e] 7.81, ^[e] 7.53 ^[e,f]	0.12	1.9×10^9	1×10^7
4,5-dihydro-3-methylfuran (3-MeDHF)	8.20, ^[e] 7.71, ^[e] 7.48 ^[e,f]	0.15	1.6×10^9	1×10^5
4,5-dihydro-2,3-dimethylfuran (2,3-Me ₂ DHF)	7.86, ^[e] 7.45, ^[e] 7.17 ^[e,f]	0.20	3.6×10^9	1.9×10^4
3,4-dihydro-2H-pyran	8.36 ^[d]	0.23	5.9×10^8	6×10^6
D-galactal	9.0 ^[e]		5.2×10^7	$> 5 \times 10^7$

[a] Vertical ionization potential. [b] Using I^- for actinometry and taking $\Phi(e^-)_{222\text{ nm}}$ from I^- to be 0.27.^[10] [c] Shown for comparison. [d] From ref[11]. [e] From DFT calculations, see text for details. [f] Adiabatic ionization potential. [g] This work. From PES. [h] Determined optically. DME⁺ was produced by reaction with $\text{N}_3^{\cdot-}$. [i] Determined optically. DME⁺ produced by reaction with $\text{Br}_2^{\cdot-}$. [j] From ref[12].

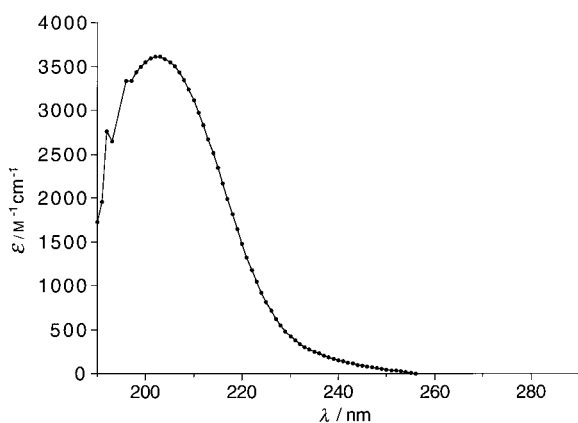
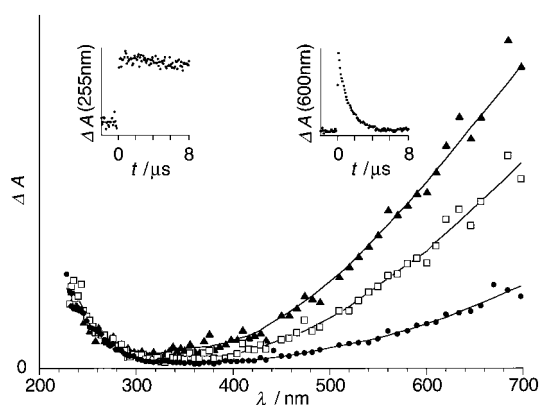
Figure 1. Absorption spectrum of 4,5-dihydro-2,3-dimethylfuran in H_2O .

Figure 2. Absorption spectra observed on photolysis at 222 nm of *t*BuOCH=CH₂ (6 mM) in H_2O , pH 10.1, recorded at 0.4 (\blacktriangle), 0.8 (\square), and 2 μs (\bullet) after the pulse. In the insets it is seen that the lifetime of e^-_{aq} (monitored at 600 nm) is considerably shorter than that of the water adduct(s) to the radical cation (monitored at 255 nm).

phase vertical IP of 8.8 eV. Since the photon energy of 222 nm light corresponds to 5.59 eV, at least 3.2 eV of additional free energy is required in this case to enable the ionization process. In fact, it is known that up to 3.5 eV are available from

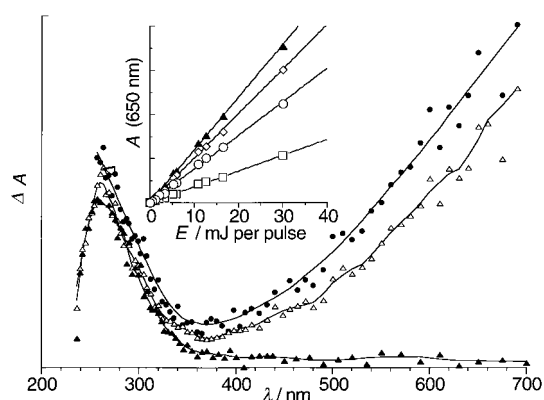


Figure 3. Absorption spectra observed at 0.8 μs (\bullet) and 4 μs (\blacktriangle) on photolysis at 222 nm of *cis*-dimethoxyethene (1.1 mM) in H_2O . \blacktriangle represents the spectrum recorded at 4 μs after addition of 2-chloroethanol (150 mM) to scavenge e^-_{aq} . The inset shows the dependence on laser power at 222 nm of the yield of e^-_{aq} , monitored at 650 nm, for a series of enoethers: \square = *cis*-dimethoxyethene, \circ = ethyl-1-propenylether, \diamond = 4,5-dihydro-2H-pyran, \blacktriangle = actinometry (KI).^[10]

the hydration of the ions produced in the photo-induced electron loss.^[13, 14] The rate of hydration of e^- has been determined to be $\geq 3 \times 10^{12} \text{ s}^{-1}$,^[15, 16] so the hydration of the electron and the corresponding release of energy can be considered to be synchronous with the ionization.

As seen in Figure 2 and Figure 3, in addition to the absorption due to e^-_{aq} , there is a band at 220–240 nm, which is assigned to the radical cation, EE^+ , or, if the radical cation is very short-lived (as in the case of *tert*-butoxyethene), to its follow-up products (\equiv FP) (see below). By comparing the optical density at 220–240 nm with that due to e^-_{aq} at 600 nm, and by taking into account that $[\text{EE}^+] = [e^-_{\text{aq}}]$ and $\epsilon(e^-_{\text{aq}})_{600\text{ nm}} = 13300 \text{ M}^{-1}\text{cm}^{-1}$,^[17] the ϵ values of EE^+ or their follow-up products^[18] were calculated and are presented in column 3 or 5, respectively, of Table 2.

Generation of EE^+ using oxidizing radicals: As an alternative to the photochemical production of EE^+ , a radiation-chemical approach was taken. In aqueous solution, ionizing

Table 2. λ_{\max} Values and extinction coefficients of $EE^{+\cdot}$ and of FP (error limits $\pm 10\%$)

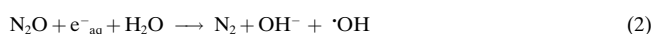
Enolether	$\lambda_{\max}(EE^{+\cdot})$ [nm]	$\epsilon(EE^{+\cdot})$ [$M^{-1}cm^{-1}$]	$\lambda_{\max}(FP)$ [nm]	$\epsilon(FP)$ [$M^{-1}cm^{-1}$]
<i>tert</i> -butyl vinyl ether			238, 236 ^[a]	2000, 2100 ^[a]
ethyl-1-propenyloxy ether	246	9700	229, 233, ^[b] 233 ^[a]	2600, 2400, ^[b] 2400 ^[a]
<i>o</i> - <i>trans</i> -methoxystyrene	375	11300	309, 315 ^[b] 314 ^[a]	2800, 3350, ^[a] 3000 ^b
2,3-dihydrofuran	244	2400	248, 253, ^[b] 248 ^[a]	1900, 1700, ^[b] 1800 ^[a]
4,5-dihydro-2-methylfuran	240	4300	251, 253, ^[b] 253 ^[a]	3300, 2800, ^[b] 2800 ^[a]
4,5-dihydro-3-methylfuran	252	7700	254, 257 ^[a]	3960, 3950 ^[a]
4,5-dihydro-2,3-dimethylfuran	256, 262, ^[b] 262 ^[a]	5040, 4000, ^[b] 4000 ^[a]	244	1700
3,4-dihydro-2 <i>H</i> -pyran	254	2700	250, 250 ^b , 246 ^[a]	2200, 1800 ^b , 1800 ^[a]
2,3-dihydro-1,4-dioxene	258, 264 ^[a]	4050, 3900 ^[a]	258	2400
<i>cis</i> -dimethoxyethene	265, 264, ^[b] 267 ^[a]	5900, 5300, ^[b] 5500 ^[a]		
tetraethoxyethene	286, 282, ^[b] 281 ^[a]	5400, 5800, ^[b] 6400 ^[a]	288	3300

[a] Data from pulse radiolysis experiments involving $SO_4^{\cdot-}$ to oxidize the EE (see [Eq. (6)]). [b] From the reaction of $N_3^{\cdot-}$ (pulse radiolysis) with the EE (see [Eq. (5)]).

radiation produces the radicals $\cdot OH$ and e^-_{aq} (90%) and H^{\cdot} (10%) [Eq. (1)].



e^-_{aq} can be scavenged by N_2O to give another $\cdot OH$ as in Equation (2)



Since the strongly oxidizing radical $\cdot OH$ typically prefers to react by addition^[19] it is necessary to convert it into a species that has a higher tendency to react by electron transfer. Typically diffusion-controlled reaction with X^- ($= Br^-, SCN^-,$ or N_3^-) as outlined in Equation (3) is a means to achieve this.



For $X^- = Br^-$ or SCN^- , the final species is a dimeric radical anion formed as shown in Equation (4).



Since in N_2O -saturated X^- -containing solutions (10–100 mM), reactions 2–4 are complete in < 100 ns, it is X^{\cdot} or $X_2^{\cdot-}$ which are the species that react with added organic substrates such as EE [Eq. (5)].



A way to generate the oxidizing radical $SO_4^{\cdot-}$ takes advantage of the reducing properties of e^-_{aq} [Eq. (6)].



An example for the oxidation of an enolether by $SO_4^{\cdot-}$ is given in Figure 4 which involves $(EtO)_2C=C(OEt)_2$ ($\equiv TEE$). From the insets it is evident that the decline of the concentration of $SO_4^{\cdot-}$ (at $\lambda = 450$ nm, inset b) is accompanied by the buildup of a species with $\lambda_{\max} \approx 290$ nm (inset a), which is assigned to the radical cation of TEE, $TEE^{+\cdot}$, whose decay

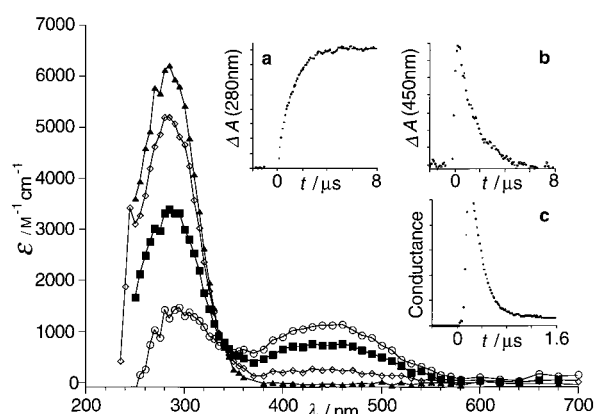


Figure 4. Reaction of $SO_4^{\cdot-}$ (generated by reaction of e^-_{aq} with $K_2S_2O_8$ (10 mM) in the presence of *tert*-butyl alcohol (0.1 M) and HPO_4^{2-} (0.5 mM) at pH 8.1) with $(EtO)_2C=C(OEt)_2$ (0.16 mM). Spectra recorded at 0.3, 2.3, and 7.8 μs after the pulse. For details on Inset a and b see text. Inset c shows the conductance change on pulse radiolysis of an N_2O -saturated solution containing N_3^- (2 mM) and TEE (0.25 mM) at pH 10.

(by reaction with water, [Eq. (7)], inset c) at pH 10 leads to a decrease of conductance (due to neutralization of OH^- by the H^+ produced).



In an analogous way, from the dependence on [EE] of the rates of buildup at $\lambda < 300$ nm or that of the decay of $SO_4^{\cdot-}$ at 450 nm the rate constants for reaction of $SO_4^{\cdot-}$ with the enolethers given in Scheme 3 were obtained, the average rate constant being $k = (4.2 \pm 1.8) \times 10^9 M^{-1} s^{-1}$. This independence of k on the structure of the EE is a reflection of the large oxidizing potential of $SO_4^{\cdot-}$ ($E = 2.6$ V/NHE^[20]). In the case of the weaker oxidant $Br_2^{\cdot-}$ ($E = 1.66$ V/NHE),^[21] the average rate constant is lower ($k = (1.1 \pm 0.97) \times 10^9 M^{-1} s^{-1}$, see Table 1) and the dependence on structure of the EE or its IP is more pronounced.

In the case of the longer lived radical cations, their extinction coefficients were measured by comparing the optical densities at $\lambda < 300$ nm after the complete decay of $SO_4^{\cdot-}$ with the dosimetry values or with that of $SO_4^{\cdot-}$ at 450 nm ($\epsilon = 1450 \pm 120 M^{-1} cm^{-1}$).^[22] The resulting numbers, reported in column 3 of Table 2, are in satisfactory agreement

with the corresponding ones obtained by using the other methods.

Lifetimes of EE^{+} in water

The rate constants for the decay of EE^{+} in water at pH 5.5–6.5 were determined partly by monitoring as a function of time their absorption at λ_{\max} or by measuring the rise in conductance on photoionization at 222 nm of the parents at pH 5.5–6.5, using time-resolved AC and, mainly DC conductance. In Figure 5 shows the situation observed with ω -methoxystyrene ($\equiv \omega$ MS) in the presence of 2-chloroethanol

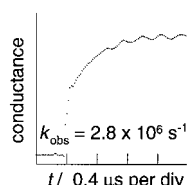


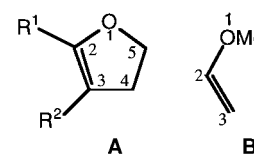
Figure 5. Conductance change on photolysis at 222 nm of an aqueous solution of PhCH=CHOMe at pH 6 which contained 2-chloroethanol (120 mM) as an electron scavenger.

as the electron scavenger. There is an initial, “fast” rise of conductance which is due to the formation of ω MS $^{+}$ and of an equivalent of Cl $^{-}$, due to dissociative dechlorination of 2-chloroethanol by e $^{-}_{aq}$ (from the photoionization), and there is a slower “follow-up reaction” with the first-order rate $2.8 \times 10^6 \text{ s}^{-1}$. The latter is identified in terms of addition of water to the β -carbon atom of the olefinic bond^[23] of ω MS $^{+}$ to give a benzyl-type radical and H $^{+}$, whose mobility is much higher than that of ω MS $^{+}$. That the ion produced in the follow-up reaction is in fact H $^{+}$ was proven by the *negative* conductance signal (not shown) obtained on performing the reaction in the presence of OH $^{-}$ (pH 9–10), where [OH $^{-}$] decreases as a result of neutralization by H $^{+}$.

As is evident from Table 1, column 5, the rate constants for the reaction of EE^{+} with H $_2$ O (or, if possible, for deprotonation from C $_{\gamma}$, see EPR section) increase with increasing IP of the EE, that is, with decreasing stability of the radical cation. Interesting is the effect of ring-size or alkylation. The additional methylene group (i.e., going from DHF to dihydropyran) leads to a decrease in the reactivity by a factor of 2; in comparison, the effect on reactivity of a methyl group at the olefinic bond is strongly dependent on its position:^[24] If Me sits at C2, there is a decrease in the reactivity by only 17%; however, if the Me group is attached to C3, the reactivity decreases by a factor of 120. Methylation at C2 of 4,5-dihydro-

3-methylfuran, that is, going to dimethyldihydrofuran, leads to a further decrease in reactivity, but only by a factor of 5. This all indicates that C3, rather than C2, is probably the site of reaction of the EE^{+} .^[25]

To obtain information on the reasons for this reactivity difference between C2 and C3, MO calculations were performed on the dihydrofurans **A** (DHF: R 1 = R 2 = H; 2-MeDHF: R 1 = Me, R 2 = H; 3-MeDHF: R 1 = H, R 2 = Me; 2,3-Me $_2$ DHF: R 1 = R 2 = Me) and on the very simple model **B**.



The ionization potentials of the EEs are also obtained from the DFT calculations. These values are reported in Table 1, together with the experimentally determined numbers. It is evident that in all cases the calculated IPs are *lower* than the experimental ones, which seems to be a general trend for the B3LYP method.^[26] The calculated spin and charge densities and the differential charge densities (C2 and C3) of the radical cations are reported in Table 3.

With all the EE^{+} values in Table 3 the spin is localized mainly on O1 and C3. The spin density distribution does not alter much on methylating C2, but there is a noticeable change on introducing the methyl group at C3: The spin density at C3 decreases in favor of that at C2, while that at O1 remains the same. Since methyl groups typically stabilize alkyl radicals, this phenomenon would not be understandable unless it was assumed that stabilization of the positive charge by the methyl group is relatively more important.^[27] This idea is supported by considering the *difference* in *positive charge* densities between C2 and C3 (see column 5 of Table 3). Compared to the number 0.28 for the parent (DHF) this difference *increases* on methylation of C2, but it *decreases* when the methyl group sits at C3. From the DFT data it is thus concluded that the methyl group at C3 exerts a considerable stabilization (by hyperconjugative delocalization) of the positive charge at C3. If it is now assumed that C3 is the “reactive site”^[28] and, in particular, that the reaction of EE^{+} in water proceeds by addition of H $_2$ O to C3, the very strong deactivating effect (factor 120, see Table 1) of placing a methyl group at C3 can be understood in terms of stabilization of the positive charge at C3 together with the steric hindrance for access of a water molecule to this position. Interestingly, as compared to methylation at C3, introducing a *second* methyl group (at C2), that is, going to 2,3-*dimethyl*-4,5-dihydrofuran, has only a small effect (factor 5, see column 5 of Table 1) on the lifetime of the EE^{+} .

Table 3. Spin and charge density on the O1, C2, and C3 atoms for the radical cations of the DHF compounds and of methoxyethene.^[a]

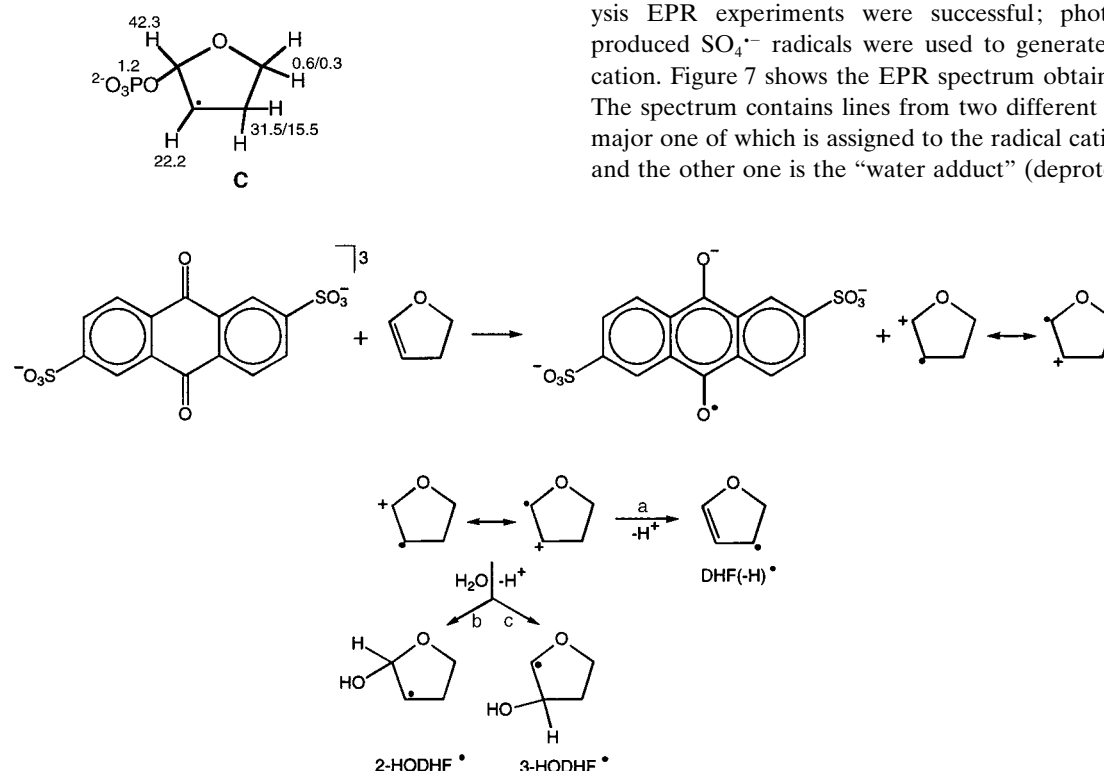
EE	Spin/charge ^[b] density on position			Difference Δ ^[c]
	O1	C2	C3	
DHF	0.30, -0.31 ^[b]	0.09, 0.24 ^[b]	0.51, -0.04 ^[b]	0.28
2-MeDHF	0.30, 0.20, ^[d] -0.35, ^[b] -0.26 ^[b,d]	0.09, 0.02, ^[d] 0.44, ^[b] 0.56 ^[b,d]	0.51, 0.81, ^[d] -0.04, ^[b] -0.06 ^[b,d]	0.48, 0.62 ^[d]
2-(HOCH $_2$)DHF	0.29, -0.35 ^[b]	0.10, 0.42 ^[b]	0.50, -0.02 ^[b]	0.44
3-MeDHF	0.33, -0.33 ^[b]	0.15, 0.24 ^[b]	0.39, 0.14 ^[b]	0.10
2,3-Me $_2$ DHF	0.28, -0.36 ^[b]	0.14, 0.45 ^[b]	0.44, 0.14 ^[b]	0.31
methoxyethene	0.37, -0.30 ^[b]	0.07, 0.23 ^[b]	0.55, -0.18 ^[b]	0.41

[a] According to the NPA method. Compared to O1 and C3, there is only little spin on the other atoms in the ring. [b] Charge density. [c] Δ is the *difference* of charge density on the C2 and C3 atoms (C2 – C3) in the radicals according to the NPA method. [d] From ref. [8b].

EPR measurements

To check these ideas and to obtain information on the nature of the products from the reaction of EE^{++} with/in water, we applied the time-resolved FT EPR technique. Aqueous solutions at $5-7^{\circ}\text{C}$ and $\text{pH} \geq 9$ that contained 10–200 mM 2,3-DHF and 1 mM anthraquinone-2,6-disulfonate (AQDS) were photolyzed with the 308 nm, 20-ns pulses from a XeCl^* excimer laser while flowing through the ≤ 1.8 mm diameter quartz tube positioned in the EPR resonator. Details of the instrument and of the technique are reported in reference [29]. Under these conditions, the 308 nm light is absorbed only by the AQDS to give its triplet state, $^3\text{AQDS}$. $^3\text{AQDS}$ is typically a strong electron acceptor^[30] that is expected to be able to abstract an electron also from EEs. In fact, at an $[\text{EE}]$ concentration of ≥ 10 mM, the life time of $^3\text{AQDS}$ was found to be ≤ 20 ns.^[31] This means that after 40 ns, the earliest time window of the apparatus (equivalent in this case to ≥ 2 reaction periods), a first meaningful recording of the situation after the pulse can be made. At this time, lines from three different radicals were found. Based on their known^[32] EPR parameters, they are identified in terms of the “water adducts” to C2 and C3, 2-HODHF \cdot and 3-HODHF \cdot (Scheme 4, steps b and c), and to the allyl-type radical DHF(-H) \cdot , formed by deprotonation (step a) of the initially produced DHF $^{++}$.^[33]

DHF $^{++}$ itself was not seen, although, according to the conductance results (Table 1), its lifetime in *dilute* aqueous solution is as large as 83 ns. When ≈ 20 mM phosphate was added to the solution at pH 9.2, there was a strong signal from the 2-phosphato-DHF-3-yl radical C ($g = 2.0034$; the coupling constants are in Gauss),^[34] which had replaced those from the



Scheme 4. Reaction of AQDS with 2,3-DHF.

water adducts, 2- or 3-HODHF \cdot . This indicates that, on the molar basis, the phosphate dianion is a much more reactive nucleophile (a high reactivity of radical cations of the enolether-type with phosphate and other nucleophiles has been previously observed.^[35–37]) than water (cf. reactivity of DME $^{++}$ and of 2,3-Me $_2$ DHF $^{++}$, see below), and that phosphate appears to react in a site-selective way (C2 is preferred over C3^[38]). If this idea is applied to the radical ion pair formed by C3'-phosphate heterolysis in DNA (Scheme 1, step a), recombination is predicted to occur, whereby addition at C3' should lead to a *reversible* situation. Concerning the possibly favored addition to C4',^[38] a question is whether this is sterically possible in DNA.

At higher concentrations of DHF (≥ 30 mM) an additional radical was seen which is assigned—on the basis of its known EPR parameters^[32]—to the dimer radical formed by electrophilic addition of DHF $^{++}$ to the DHF parent. To see a representative of EE^{++} *directly*, the long-lived (53 μs , see Table 1) radical cation of 2,3-Me $_2$ DHF was produced by using the same conditions as described for DHF. The spectrum of 2,3-Me $_2$ DHF $^{++}$ is presented in Figure 6.

The upper trace is the experimental spectrum ($g = 2.0045$), the lower trace the spectrum simulated by using the parameters $a(\text{CH}_3)_{\text{C}2} = 5.7$, $a(\text{CH}_3)_{\text{C}3} = 18.4$, $a(\text{H})_{\text{C}4} = 34.2(2)$, $a(\text{H})_{\text{C}5} = 8.2(2)$ G. On the basis of the EPR coupling constants, there is a higher unpaired spin density at C3 than at C2, which is as expected and in line with the DFT calculations (see Table 3). In the case of 2-MeDHF two radicals were identified: The water-adduct to C3 (3-HO-2-MeDHF-2-yl, main product) and the allyl radical formed by deprotonation of 2-MeDHF $^{++}$ from C4.

As a second example for a long-lived radical cation, *cis*-DME was studied. With *cis*-DME, *steady-state* in situ photolysis EPR experiments were successful; photochemically produced $\text{SO}_4^{\cdot-}$ radicals were used to generate the radical cation. Figure 7 shows the EPR spectrum obtained at pH 7: The spectrum contains lines from two different radicals, the major one of which is assigned to the radical cation, DME $^{++}$, and the other one is the “water adduct” (deprotonated from

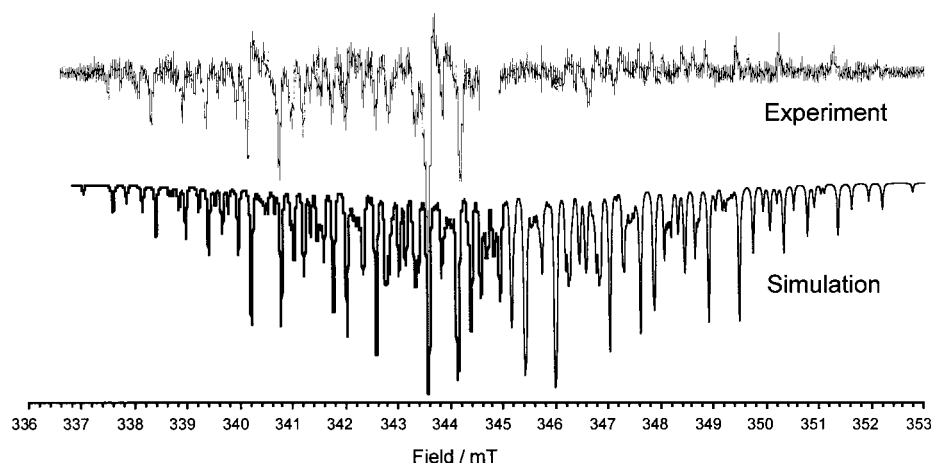


Figure 6. EPR spectrum recorded at 40 ns after photolysis (with the 308 nm pulse) of a solution of AQDS (1 mM; at pH 11) in the presence of 2,3-Me₂DHF (10 mM) at 5–7 °C.

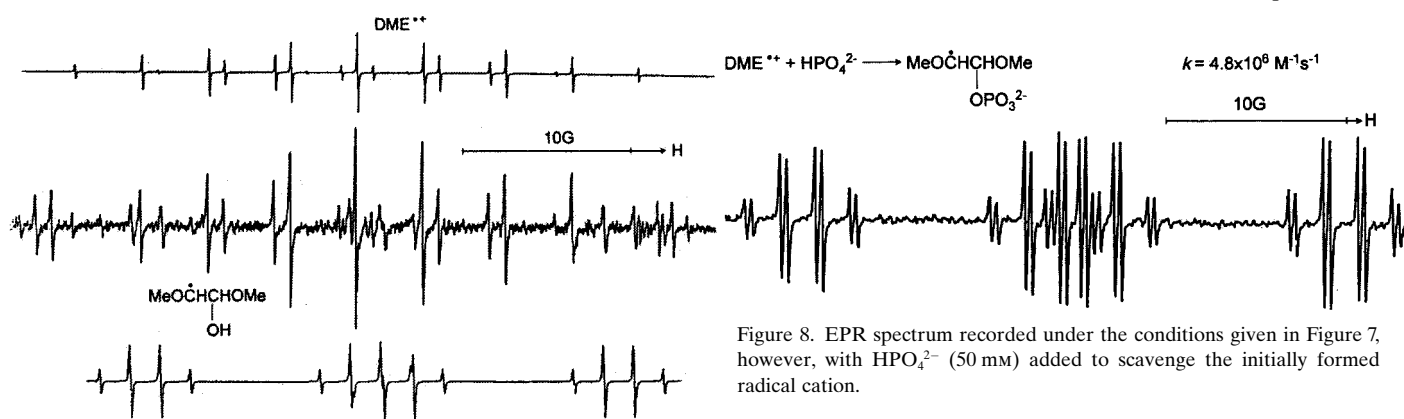


Figure 7. EPR spectrum of the radicals observed on photolysis at ≈ 250 nm of an aqueous solution containing acetone (0.3 M; as sensitizer), K₂S₂O₈ (20 mM), and *cis*-DME (0.1 mM) at 3 °C and pH 5–7.

the in-coming OH₂), MeOC·HCH(OH)OMe. The “water adduct” was independently and selectively produced at pH 6.5 by reaction of ·OH (generated by photolysis at ≈ 250 nm of H₂O₂) with DME, a result supporting the identification of the reaction product as MeOC·HCH(OH)-OMe. Clearly, C–H deprotonation of the radical cation is not a possibility in the case of DME^{•+}. The simultaneous presence of the radical cation and its reaction product, the water adduct, on the millisecond time scale characteristic of the steady-state EPR experiment is in agreement with the low rate constant for reaction of DME^{•+} with water, $k = 7.5 \times 10^3 \text{ s}^{-1}$ (Table 1).

As in the case of DHF, the reactivity of DME^{•+} was tested with a nucleophile other than the solvent. In the presence of HPO₄²⁻ (50 mM) at pH 9.2, the only lines visible (see Figure 8) were those from the “phosphate adduct”, MeOC·HCH-(OPO₃²⁻)OMe, which is formed by addition of HPO₄²⁻ to the “double bond” of DME^{•+}.

The rate constant for this reaction was determined to be $4.9 \times 10^6 \text{ M}^{-1} \text{ s}^{-1}$ by monitoring the rate of decay of DME^{•+} at 270 nm as a function of [HPO₄²⁻]. This value may be compared with the value of $6.7 \times 10^5 \text{ M}^{-1} \text{ s}^{-1}$ measured for reaction of 2,3-Me₂DHF^{•+} with the same nucleophile. The

electrophilic reactivity of DME^{•+} and of 2,3-Me₂DHF^{•+} with nucleophiles other than HPO₄²⁻ was also studied. The rate constants for reaction with acetate, carbonate and, of course, hydroxide were determined and the reactivities of these nucleophiles with the two EE^{•+}s follow a Brønsted-type relation; an example is given in Figure 9. From the slopes of the plots (which are influenced strongly by the value for OH⁻), the Brønsted coefficient is 0.35 or 0.31, respectively, indicating that the transition state for the electrophile–nu-

Figure 8. EPR spectrum recorded under the conditions given in Figure 7, however, with HPO₄²⁻ (50 mM) added to scavenge the initially formed radical cation.

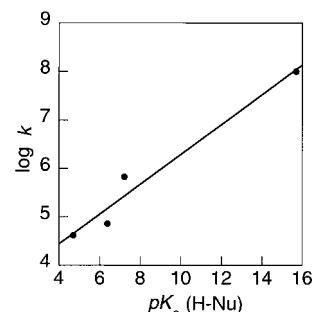


Figure 9. Dependence on $pK_a(\text{H-Nu})$ of the rate constant for the reaction of 2,3-Me₂DHF^{•+} with the nucleophiles Nu⁻, acetate, hydrogencarbonate, hydrogenphosphate, and OH⁻.

cleophile interaction is more reagent- than product-like which is in agreement with the fact that the rate constants are much below the diffusion limit.

Oxidizing properties of EE^{•+}

In the case of DME, the ability of its radical cation, DME^{•+}, to abstract an electron from electron-rich compounds such as phenols and amines could be studied easily, due to the long lifetime of DME^{•+}. The experiments were performed at pH 5.6–7.9 where DME^{•+} was produced with N₃^{•-} (see [Eq. (5)]). The data obtained are collected in Table 4.

Table 4. Rate constants for the oxidation of electron donors (D) by DME^{•+}.

e-donor D ^[a]	pK _s (D) ^[a]	E ₇ (D ^{•+} + e ⁻) [mV/NHE]	λ _{max} (D ^{•+}) [nm]	k(DME ^{•+} + D) [M ⁻¹ s ⁻¹]/pH	k(2,3-Me ₂ DHF ^{•+} + D) [M ⁻¹ s ⁻¹]/pH
TMPD		270 ^[b]	330, 565, 610	2.5 × 10 ⁹ /7.7	
L-(+)-ascorbic acid	4.10	300 ^[b]	368, 300	2.6 × 10 ⁹ /6.3	3.5 × 10 ⁹ /7.9
4- <i>N,N</i> -dimethylaminophenol		360 ^[b]	322, 500	1.5 × 10 ⁹ /6.8	
hydroquinone	10.35	460 ^[b]	320, 430	9.1 × 10 ⁸ /7.4	5.6 × 10 ⁸ /8.0
troxol	12.1	480 ^[b]	310, 430	2.6 × 10 ⁹ /6.4	3.4 × 10 ⁹ /6.8
4-methoxyphenol	10.1	600 ^[b]	302, 420	3.8 × 10 ⁸ /7.9	2.0 × 10 ⁸ /7.9
8-OH-dGuo	8.6	740 ^[c]	330, 400	8.3 × 10 ⁸ /7.6	5.6 × 10 ⁸ /7.5
tyrosine	10.1	890 ^[c]	295, 400	4.3 × 10 ⁷ /7.0	
<i>N</i> -phenylglycine	4.1, ≥ 14	890 ^[f]	340, 460	4.2 × 10 ⁹ /5.6	
<i>p</i> -chlorophenol	9.4	940 ^[e]	305, 420	3.0 × 10 ⁷ /6.9	
tryptophan	9.44	1020 ^[e]	330, 520	2.0 × 10 ⁸ /8.0	
2'-deoxyguanosine	9.6	1290 ^[h]	310, 390, 530	4.7 × 10 ⁴ [i]	

[a] Or its deprotonated form. [b] From ref. [39]. [c] From ref. [40]. [d] From ref. [40]. [e] From ref. [41]. [f] From ref. [42]. [g] From ref. [43]. [h] From ref. [7]. [i] The ET reaction is reversible, see text.

It is evident (see Table 4, column 5) that the rate constants for oxidation of the electron donors decrease with their increasing oxidation potential until, with guanosine, the electron transfer changes direction (the guanosine radical is a stronger oxidant than DME^{•+}). The data can be described (although there is considerable scatter, as can be seen from Figure 10) by the Marcus equation for which the reorganization energy λ is 16.5 kcal mol⁻¹. The scatter may be due to contributions of inner-sphere mechanisms to the overall electron transfer. One particularly conspicuous example is *N*-phenylglycine (Δ in Figure 10) which is much more reactive with DME^{•+} than it should be on the basis of its oxidation potential.

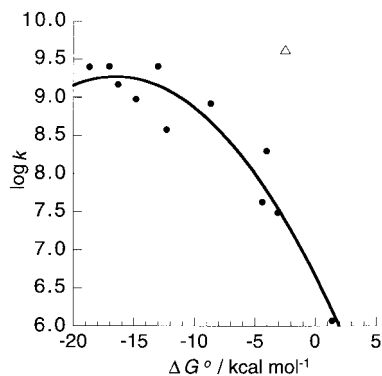
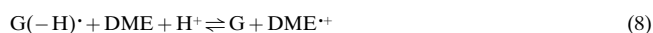


Figure 10. Marcus plot for the oxidation of the electron donors of Table 4 by DME^{•+} (Δ denotes *N*-phenylglycine; see text for details). Δ*G*[°] is the driving force for the electron transfer, assuming *E*(DME^{•+} + e⁻) = 1.08 V/NHE and taking *E*(D^{•+} + e⁻) from Table 4.

As mentioned, DME^{•+} is not able to irreversibly oxidize guanosine, the data are better explained by assuming that there is a reversible electron transfer between DME^{•+} and guanosine, the equilibrium constant for the reaction at pH 7.5 [Eq. (8)] lying on the right hand side. Since at pH 7.5, *E*(G(-H)[•] + e⁻ + H⁺) = 1.26 V/NHE,^[7] the potential for reduction of DME^{•+} must be less than this value, that is, 1.26 V is the upper limit for *E*(DME^{•+} + e⁻).



To get an estimate of the lower value, DME^{•+} was allowed to react with L(-)-tryptophan, whose oxidation potential increases with decreasing pH.^[44] DME^{•+} is able to oxidize tryptophan from pH 8 down. On reaching pH ≈ 6.2, the reaction ceased to be visible. At pH 6.2 the potential for tryptophan is 1.06 V/NHE.^[43] This number can thus be taken as an indication of the lower limit for *E*(DME^{•+}). An additional, though less useful, estimate of the lower value for the reduction potential of DME^{•+} derives from the observation that DME^{•+} is able to oxidize 4-chlorophenol (see Figure 11), whose potential is 0.94 V/NHE.^[41]

After bracketing the reduction potential of DME^{•+} as 1.06 < *E* < ≈ 1.26, experiments were performed with the aim of obtaining a more exact number. For this purpose, DME^{•+} was equilibrated with the redox standard 1,2,4-trimethoxybenzene, whose oxidation potential is 1.14 V/NHE.^[45] The radical cation of 1,2,4-trimethoxybenzene, 1,2,4-TMB^{•+}, has a strong peak at a λ_{max} of 450 nm,^[46] and it was found that it can be produced by the reaction of the radiation-chemically generated N₃[•] radical (*k* = 6.1 × 10⁹ M⁻¹s⁻¹). On addition of DME to aqueous solutions of 1,2,4-TMB under radiolysis, the lifetime of 1,2,4-TMB^{•+} was found to be drastically reduced, and its remaining concentration to depend on [DME]. The data are interpretable in terms of a reversible electron exchange between 1,2,4-TMB^{•+} and DME, the analysis of which (Figure 11) yields the value 1.09 V/NHE for the

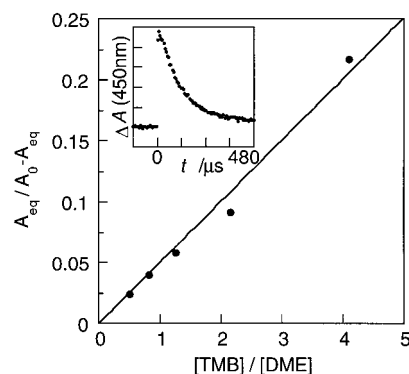


Figure 11. Dependence of the yield of 1,2,4-TMB^{•+} at equilibrium on the ratio [TMB]/[DME] in aqueous solutions containing TMB (0.5 mM) and DME (0.1–1 mM). The inset shows the decay of TMB^{•+} in a solution containing TMB (0.5 mM) and DME (1 mM) at pH 7.4.

reduction potential of $\text{DME}^{+\bullet}$ from the kinetics of approach to equilibrium^[47] and 1.06 V from the concentrations^[47] of 1,2,4-TMB^{+\bullet} at equilibrium, the average of which is 1.08 ± 0.02 V/NHE, a number close to the lower limit of the range of potential estimated above.

The attempt was made to obtain an estimate of the reduction potentials also for the radical cations of DHF and 2-MeDHF, which are better models than DME for the enolether-type radical cation formed on strand cleavage in DNA (see Scheme 1). The reduction potential of the radical cation of thioanisole ($\text{TA}^{+\bullet}$), which absorbs at $\lambda = 540$ nm, has been determined to be 1.44 V/NHE.^[48, 49] In an aqueous solution at pH 9.6, $\text{TA}^{+\bullet}$ was produced via radiation-chemically generated $\text{Br}_2^{\cdot-}$ and its decay at 540 nm monitored. DHF or 2-MeDHF was then added to this solution which led to a drastic decrease in the lifetime of $\text{TA}^{+\bullet}$. This indicates that an electron transfer reaction takes place between $\text{TA}^{+\bullet}$ and (2-Me)DHF, that is, the oxidation potentials of these enolethers are below that (1.44 V) of TA. This means that 1.44 V^[49] is the upper limit of the reduction potentials of $\text{DHF}^{+\bullet}$ or $2\text{-MeDHF}^{+\bullet}$. From plots of k_{observed} for the decay of $\text{TA}^{+\bullet}$ as a function of [DHF] or [2-MeDHF], respectively, the following rate constants were obtained: $k(\text{TA}^{+\bullet} + \text{DHF} \rightarrow \text{TA} + \text{DHF}^{+\bullet}) = 7.3 \times 10^8 \text{ M}^{-1} \text{ s}^{-1}$ and $k(\text{TA}^{+\bullet} + 2\text{-MeDHF} \rightarrow \text{TA} + 2\text{-MeDHF}^{+\bullet}) = 2.5 \times 10^9 \text{ M}^{-1} \text{ s}^{-1}$, indicating that methylation leads to a decrease of the reduction potential of the $\text{DHF}^{+\bullet}$ moiety like it leads to a decrease of the IP (see Table 1).

To get an estimate of the lower limit of the oxidation potentials of DHF and 2-MeDHF, their reactivity was tested with the 2'-deoxyguanosine radical ($\text{G}(-\text{H})^{\cdot}$),^[50] whose reduction potential at pH 7.3 is 1.27 V/NHE.^[7] $\text{G}(-\text{H})^{\cdot}$ was produced via radiation-chemically generated $\text{Br}_2^{\cdot-}$ in an aqueous solution at pH 7.3, where the decay of $\text{G}(-\text{H})^{\cdot}$ proceeded with $k \approx 2 \times 10^3 \text{ s}^{-1}$. Then, DHF was added to the solution. It was found that up to 8 mM, DHF had no effect on the lifetime of $\text{G}(-\text{H})^{\cdot}$. Thus, the oxidation potential of DHF is above 1.27 V/NHE. The rate constant for the hypothetical reaction $\text{G}(-\text{H})^{\cdot} + \text{DHF} \rightarrow \text{G} + \text{DHF}^{+\bullet}$ can be estimated as $< 2 \times 10^3 \text{ s}^{-1} / 8 \times 10^{-3} \text{ M} = 2.5 \times 10^5 \text{ M}^{-1} \text{ s}^{-1}$. To summarize the results obtained with TA and 2'-deoxyguanosine as "redox indicators", the potential $E(\text{DHF}^{+\bullet} + e^-)$ is likely to lie between 1.27 and 1.44 V/NHE.

A relevant question is to which extent DHF can be considered to be a good model for the enolether produced in the strand breakage of DNA (Scheme 1). The key here is judging the electronic effect on the potential of the enolether function of the $\text{OPO}_2\text{-OCH}_2$ group (as a substituent at C2)^[38] as compared to that of the hydrogen in DHF. At the present stage, we do not have any direct information on this. Nonetheless, on the basis of the rate constants for reaction with/in water of the radical cations of dihydropyran ($k = 6.6 \times 10^6 \text{ s}^{-1}$, see Table 1) and D-galactal ($> 5 \times 10^7 \text{ s}^{-1}$) it is reasonable to assume that OH groups (as in galactal, as models for the $\text{OPO}_2\text{-OCH}_2$ group) decrease, through their inductive effect, the stability of the enolether function which thereby becomes more electrophilic (=reactive with nucleophiles such as water) and, probably, a stronger oxidant. This means that the oxidation potential of the enolether is likely to increase as a result of the inductive effect of OH, even if OH

sits at a remote position relative to the enolether function. The relatively very high IP of galactal (9 eV, see Table 1) supports this assumption.

Conclusion

Enolether radical cations ($\text{EE}^{+\bullet}$) were generated in aqueous solution by photoionization ($\lambda \leq 222$ nm) or by electron transfer to radiation-chemically produced oxidizing radicals. The $\text{EE}^{+\bullet}$ exhibit electrophilic reactivity with respect to nucleophiles such as water or phosphate as well as electron transfer reactivity towards one-electron reductants such as phenols, amines, or ascorbic acid or vitamin E. In the case of the more long-lived enolether radical cation $\text{DME}^{+\bullet}$, it was possible to measure the reduction potential as 1.08 ± 0.02 V/NHE. In the case of the biologically more important radical cation $\text{DHF}^{+\bullet}$, the reduction potential could be bracketed as $1.29 < E < 1.44$ V/NHE. This range may serve as a guide for the oxidizing power of the enolether-type radical cation produced^[2] (Scheme 1) on heterolysis of the C4' radical in DNA. On the basis of their relatively high oxidation potential,^[51] the enolether radical cations are strong oxidants which are clearly able^[52] to oxidize the DNA base guanine ($E(\text{dG}(-\text{H})^{\cdot} + e^- + \text{H}^+)_{\text{pH}7} = 1.29$ V/NHE)^[7] and they may even be able to oxidize the nucleoside adenosine ($E(\text{dA}(-\text{H})^{\cdot} + e^- + \text{H}^+) = 1.42$ V/NHE).^[7] An aspect related to their relatively high electron deficiency is their pronounced tendency to react as electrophiles (with respect to nucleophiles such as water, phosphate, or hydroxide) or as Brønsted acids (if there exists a $\text{C}_\gamma\text{-H}$). In real life situations, such as in DNA in aqueous solution, this electrophilic reactivity^[2] competes with the one-electron transfer chemistry.

Experimental Section

General: Except 3-methyl- and 2,3-dimethyl-3,4-dihydrofuran, the enolethers were purchased from Aldrich and Fluka. They were distilled over Na (to remove OH-containing compounds and traces of acid which could lead to decomposition) to a purity $\geq 99.8\%$. 3-Methyl-^[53-55] and 2,3-dimethyl-3,4-dihydrofuran^[56, 57] were prepared according to literature procedures and purified by distillation to $\geq 99\%$. All other chemicals were of the highest purity commercially available and used as received. The quantum yields for photoionization by the 222 nm laser light were determined with reference to an aqueous solution of KI for which $\Phi(e^-) = 0.27$.^[10] The vertical ionization potentials were determined at room temperature by the photoelectron spectroscopy (PES) method, for which a Perkin-Elmer PS 18 spectrometer was used. The calibration was performed with Ar (15.76 and 15.94 eV) and Xe (12.13 and 13.44 eV). The resolution was 20 meV as judged by the $^3\text{P}_{3/2}$ Ar line.

Pulse radiolysis experiments: A 3 MeV van de Graaff accelerator was used that delivered 100–400 ns pulses with doses such that $0.5\text{--}2 \mu\text{M}$ radicals were produced. The optical or conductance (AC or DC) traces were recorded with Tektronix 7612 or 7912 transient digitizers and transferred to a DEC LSI11-73+ computer which also process-controlled the apparatus and preanalyzed the experimental data on-line. Dosimetry was performed with N_2O -saturated aqueous 10 mM KSCN solutions in which the radiation produces, with a yield of $G = 6$, the radical $(\text{SCN})_2^{\cdot-}$ whose ϵ value is $7600 \text{ M}^{-1} \text{ cm}^{-1}$ at its λ_{max} of 480 nm.^[58] For the time-resolved photolysis experiments, a Lambda Physik EMG MSC excimer laser was used which delivered 20 ns pulses of 193 nm (ArF*) or 222 nm (XeF*) light with

energies of 10–50 mJ per pulse. The light-induced signals were recorded and processed the same way as in the case of the pulse radiolysis.

MO calculations: The energy calculations and geometry optimizations were carried out with the GAUSSIAN 98 program package^[59] utilizing density functional theory (DFT) with an unrestricted wave function. The functional employed was the Lee, Yang, and Parr for the correlation part^[60] and Becke's three parameter one for the exchange part (B3LYP).^[61, 62] The split valence standard 6–31G(d) basis set^[63] was used in all the calculations. Charge and spin densities were analyzed by Mulliken^[64] and NPA (natural population analysis, which is based on the natural bond order theory^[65])^[66] methods, which gave very similar results.

Acknowledgement

We thank the Volkswagenstiftung (project I/72040) for a scholarship (K.B.) and the additional financial support.

- [1] For a recent review, see: M. Bietti, S. Steenken in *Handbook of Electron Transfer* (Ed.: V. Balzani) Wiley-VCH, Weinheim 2001, pp. 494–579.
- [2] M. Dizdaroglu, C. von Sonntag, D. Schulte-Frohlinde, *J. Am. Chem. Soc.* **1975**, *97*, 2277–2278.
- [3] C. von Sonntag, U. Hagen, A. Schön-Bopp, D. Schulte-Frohlinde, *Adv. Radiat. Biol.* **1981**, *6*, 109–142.
- [4] B. Giese, S. Wessely, M. Spormann, U. Lindemann, E. Meggers, M. E. Michel-Beyerle, *Angew. Chem.* **1999**, *111*, 1050–1052; *Angew. Chem. Int. Ed.* **1999**, *38*, 996–998.
- [5] The third characteristic reaction is C–H deprotonation which has been described for enolether radical cations in references [6] and [32].
- [6] B. Giese, X. Beyrich-Graf, P. Erdmann, M. Petretta, U. Schwitter, *Chem. Biol.* **1995**, *2*, 367–375.
- [7] S. Steenken, S. V. Jovanovic, *J. Am. Chem. Soc.* **1997**, *119*, 617–618.
- [8] Radical cations of model enolethers have recently been produced by a photochemically induced heterolytic β -fragmentation reaction, see: a) M. Newcomb, N. Miranda, X. H. Huang, D. Crich, *J. Am. Chem. Soc.* **2000**, *122*, 6128–6129; b) R. Glatthar, M. Spichty, A. Gugger, R. Batra, W. Damm, M. Mohr, H. Zipse, B. Giese, *Tetrahedron* **2000**, *56*, 4117–4128.
- [9] M. Hesse, H. Meier, B. Zeeh, *Spektroskopische Methoden in der organischen Chemie*, Thieme, Stuttgart, **1995**.
- [10] A. Iwata, N. Nakashima, M. Kusaba, Y. Izawa, C. Yamanaka, *Chem. Phys. Lett.* **1993**, *207*, 137–142.
- [11] S. G. Lias, J. F. Liebman, R. D. Levin, S. A. Kafafi, NIST Standard Reference Database 25, Structures and Properties, Version 2.02, National Institute of Standards and Technology, Gaithersburg, MD 20899 **1994**.
- [12] N. Zeug, J. Bücheler, H. Kisch, *J. Am. Chem. Soc.* **1985**, *107*, 1459–1465.
- [13] M. Braun, J. Y. Fan, W. Fuss, K. L. Kompa, G. Müller, W. E. Schmid, "UV Laser Ionization Spectroscopy and Ion Photochemistry" in *Methods in Laser Spectroscopy* (Eds.: Z. Prior, A. Ben-Reuven, M. Rosenbluh), Plenum Press, New York, **1986**, p. 367–378.
- [14] The largest contribution to the heat of hydration is due to the photoejected electron, rather than to the much larger organic radical cation.
- [15] J. M. Wiesenfeld, E. P. Ippen, *Chem. Phys. Lett.* **1980**, *73*, 47–50.
- [16] Y. Gauduel, H. Gelabert, M. Ashokkumar, *Chem. Phys.* **1995**, *197*, 167–193.
- [17] G. L. Hug, *Optical spectra of nonmetallic inorganic transient species in aqueous solution*, Vol. 69, Nat. Stand. Ref. Data Ser., Nat. Bur. Stand. (U. S.), **1981**.
- [18] To determine the ϵ value of EE^{++} , the end-of-pulse optical density (at about 50 ns) was recorded; to obtain that of FP, the optical density at the end of the first order decay of EE^{++} was measured.
- [19] S. Steenken, *J. Chem. Soc. Faraday Trans. 1* **1987**, *83*, 113–124.
- [20] L. Ebersson, *Electron Transfer Reactions in Organic Chemistry*, Vol. 25, Springer, Berlin **1987**.
- [21] P. Wardman, *J. Phys. Chem. Ref. Data* **1989**, *18*, 1637–1755.
- [22] J. L. Faria, S. Steenken, *J. Phys. Chem.* **1992**, *96*, 10869–10874.
- [23] O. Brede, F. David, S. Steenken, *J. Chem. Soc. Perkin Trans. 2* **1995**, 23–32.
- [24] Interestingly, the effect of methylation at C2 or at C3 on the (gas-phase) ionization potentials is negligible, see column 2 of Table 1.
- [25] A similar result (on 2-MeDHF⁺⁺) has been obtained by B. Giese et al.^[8b]
- [26] B. S. Jursic, *J. Chem. Soc. Perkin Trans. 2* **1996**, 697–700; H. M. Muchall, N. H. Werstiuk, B. Choudhury, *Can. J. Chem.* **1998**, *76*, 221–227; S. D. Wetmore, R. J. Boyd, L. A. Eriksson, *J. Phys. Chem. B* **1998**, *102*, 5369–5377; S. D. Wetmore, R. J. Boyd, L. A. Eriksson, *J. Phys. Chem. B* **1998**, *102*, 10602–10614; S. D. Wetmore, R. J. Boyd, L. A. Eriksson, *J. Phys. Chem. B* **1998**, *102*, 9332–9343
- [27] It is known (P. Vogel, *Carbocation Chemistry*, Vol. 21, Elsevier, Amsterdam, **1985**) that alkyl groups stabilize carbocations much more than radicals.
- [28] Using 2-MeDHF⁺⁺ as a model, and product analysis as a tool, it was shown that C3 is the preferred site for the addition of H₂O.^[8b]
- [29] T. Kausche, J. Säuberlich, E. Trobitzsch, D. Beckert, K.-P. Dinse, *Chem. Phys.* **1996**, *208*, 375–390.
- [30] J. Geimer, D. Beckert, *J. Phys. Chem. A* **1999**, *103*, 3991–3998, and references therein.
- [31] The rate constant for reaction of ³AQDS with DHF was measured by monitoring the decay of ³AQDS at 380 nm as a function of [DHF] to be $5.0 \times 10^9 \text{ M}^{-1} \text{ s}^{-1}$.
- [32] B. C. Gilbert, R. O. C. Norman, P. S. Williams, *J. Chem. Soc. Perkin Trans. 2* **1980**, 647–656.
- [33] The "water adducts", 2- and 3-HODHF[•], can probably be reconverted to the radical cation by H⁺-induced dehydration, which is the reverse of the "hydration reaction", as has been observed in the case of 2,3-dihydro-1,4-dioxene.^[1]
- [34] Interestingly, the 2-yl radical expected from addition of HPO₄²⁻ to the C3 position of DHF⁺⁺ was not seen.
- [35] Phosphate has a high reactivity also in the case of 1,1-dialkoxyalkene radical cations, see: G. Behrens, E. Bothe, G. Koltzenburg, D. Schulte-Frohlinde, *J. Chem. Soc. Perkin Trans. 2* **1980**, 883–889 and references [39] and [41].
- [36] G. Behrens, E. Bothe, G. Koltzenburg, D. Schulte-Frohlinde, *J. Chem. Soc. Perkin Trans. 2* **1981**, 143–154.
- [37] G. Trampe, J. Mattay, S. Steenken, *J. Phys. Chem.* **1989**, *93*, 7157–7160.
- [38] The numbering here is different from that in DNA: In the DHFs, C2 corresponds to C4' in DNA.
- [39] S. Steenken, P. Neta, *J. Phys. Chem.* **1982**, *86*, 3661–3667.
- [40] S. Steenken, S. V. Jovanovic, M. Bietti, K. Bernhard, *J. Am. Chem. Soc.* **2000**, *122*, 2373–2374.
- [41] J. Lind, X. Shen, T. E. Eriksen, G. Merenyi, *J. Am. Chem. Soc.* **1990**, *112*, 479–482.
- [42] M. Canle Lopez, J. A. Santaballa, S. Steenken, *Chem. Eur. J.* **1999**, *5*, 1192–1201.
- [43] A. Harriman, *J. Phys. Chem.* **1987**, *91*, 6102–6104.
- [44] S. V. Jovanovic, S. Steenken, *J. Phys. Chem.* **1992**, *96*, 6674, and references therein.
- [45] M. Bietti, E. Baciocchi, S. Steenken, *J. Phys. Chem. A* **1998**, *102*, 7337–7342.
- [46] P. O'Neill, S. Steenken, D. Schulte-Frohlinde, *J. Phys. Chem.* **1975**, *79*, 2773–2779.
- [47] S. Steenken, P. Neta, *J. Phys. Chem.* **1979**, *83*, 1134–1137.
- [48] M. Jonsson, J. Lind, G. Merenyi, T. E. Eriksen, *J. Chem. Soc. Perkin Trans. 2* **1995**, 67–70.
- [49] We have recently obtained evidence for the reduction potential of TA⁺⁺ to be even higher: 1.5 V/NHE.
- [50] L. P. Candeias, S. Steenken, *J. Am. Chem. Soc.* **1989**, *111*, 1094–1099.
- [51] Compared with other "biological oxidants" such as tyrosyl ($E = 0.93 \text{ V}^{[43]}$), tryptophyl ($1.01–1.08 \text{ V}^{[43, 44]}$), or thyl radicals (0.75 V).
- [52] B. Giese, *Acc. Chem. Res.* **2000**, *33*, 631–636.
- [53] D. J. Collins, A. M. James, *Aust. J. Chem.* **1989**, *42*, 223–228.
- [54] A. Schmitt, H.-U. Reißig, *Chem. Ber.* **1995**, *128*, 871–876.
- [55] O. Temme, S.-A. Taj, P. G. Andersson, *J. Org. Chem.* **1998**, *63*, 6007–6015.
- [56] D. E. McGreer, N. W. K. Chiu, M. G. Vinje, *Can. J. Chem.* **1965**, *43*, 1398–1405.
- [57] K. Gollnik, K. Knutzen-Mies, *J. Org. Chem.* **1991**, *56*, 4017–4027.

- [58] R. H. Schuler, A. L. Hartzell, B. Behar, *J. Phys. Chem.* **1981**, *85*, 192–199.
- [59] M. J. Frisch, G. W. Trucks, H. B. Schlegel, G. E. Scuseria, M. A. Robb, J. R. Cheeseman, V. G. Zakrzewski, J. A. Montgomery, R. E. Stratmann, J. C. Burant, S. Dapprich, J. M. Millam, A. D. Daniels, K. N. Kudin, M. C. Strain, O. Farkas, J. Tomasi, V. Barone, M. Cossi, R. Cammi, B. Mennucci, C. Pomelli, C. Adamo, S. Clifford, J. Ochterski, G. A. Petersson, P. Y. Ayala, Q. Cui, K. Morokuma, D. K. Malick, A. D. Rabuck, K. Raghavachari, J. B. Foresman, J. Cioslowski, J. V. Ortiz, B. B. Stefanov, G. Liu, A. Liashenko, P. Piskorz, I. Komaromi, R. Gomperts, R. L. Martin, D. J. Fox, T. Keith, M. A. Al-Laham, C. Y. Peng, A. Nanayakkara, C. Gonzalez, M. Challacombe, P. M. W. Gill, B. Johnson, W. Chen, M. W. Wong, J. L. Andres, M. Head-Gordon, E. S. Replogle, J. A. Pople, Gaussian 98, Gaussian Inc., Pittsburgh **1998**.
- [60] C. Lee, W. Yang, R. G. Parr, *Phys. Rev. B.* **1988**, *37*, 785–789.
- [61] A. D. Becke, *Phys. Rev. A.* **1988**, *38*, 3098–3100.
- [62] A. D. Becke, *J. Chem. Phys.* **1993**, *98*, 5648–5652.
- [63] P. C. Hariharan, J. A. Pople, *Theoret. Chim. Acta* **1973**, *28*, 213–222.
- [64] R. S. Mulliken, *J. Chem. Phys.* **1962**, *36*, 3428–3439.
- [65] J. P. Foster, F. Weinhold, *J. Am. Chem. Soc.* **1980**, *102*, 7211–7218.
- [66] A. E. Reed, L. A. Curtiss, F. Weinhold, *Chem. Rev.* **1988**, *88*, 899–926.

Received: February 19, 2001 [F3081]